Geometry-Based Automated Recognition of Objects on Satellite Images of Sub-meter Resolution

D. K. Mozgovoy[1[0000-0003-1632-1565]], D. V. Kapulin[2[0000-0002-4260-1408]], D. N. Svinarenko[1[0000-0003-3179-9129]], T. N. Yamskikh[2[0000-0002-5658-6632]], A. A. Chikizov[2[0000-0002-8076-9244]] and R. Yu. Tsarev[2[0000-0002-6740-1840]]

[1] Oles Honchar Dnipro National University, 72, Gagarin Prospect, Dnipro, 49000, Ukraine
[2] Siberian Federal University, 79, Svobodny Prospect, Krasnoyarsk, 660041, Russia
tsarev.sfu@mail.ru

Abstract. The paper considers an algorithm for automated classification of mobile small size objects on multispectral satellite images of submeter spatial resolution using radiometric and geometric features. It ensures recognizing the desired classes of objects with high accuracy regardless of their orientation in the image. The geometric features of the objects classified in the binary image included the area of the object, the lengths of the principal and auxiliary axes of inertia, the eccentricity of the ellipse with the main moments of inertia, the area of a convex polygon described near the object, the equivalent diameter of a circle with the same area, and the convexity coefficient.

Keywords: Satellite Monitoring, Sub-meter Resolution, Image Processing.

1 Introduction

The most difficult task in automated processing of multispectral satellite images of sub-meter spatial resolution is searching and recognizing small objects (structures, vehicles, etc.) using radiometric, spectral, textural, statistical, geometric, and other decoding features [1-3]. The values of the upper and lower binarization threshold (so-called cut-off threshold) are usually used as radiometric decoding features for each spectral channel of the image, which are selected manually or read from the decryption feature library file. Geometric characteristics include area, perimeter, shape coefficient, describing the roundness and convexity of the object, eccentricity, center of gravity, coordinates of the describing rectangle, etc [4-6].

Most of the existing modern software packages for processing satellite images ensure per-pixel classification of images or areas of interest in general, as a rule, taking into account only their spectral characteristics, without analyzing the geometric properties of separate objects [7-9]. Skeleton-based methods to determine geometric parameters of objects in binary images, (e.g., used in character recognition), are not invariant with respect to rotation and therefore cannot be used to recognize moving objects with arbitrary orientation [10-12]. Recognition methods using neural networks developed in recent years require long term training, as well as high requirements for computing resources [13-15].

The research was aimed at developing and subsequent testing the methods and algorithms for automated classification of small objects on multispectral satellite images of sub-meter spatial resolution using geometric features invariant to rotation.

2 Mathematical models and methods

The simplest and most common geometric features that are invariant to rotation are the area and perimeter of the object.

The pixel area of a binary object is equal to the number of nonzero image elements belonging to the object. Moreover, the set of single readings (x, y) with coordinates (x, y) belonging to the region A is given as follows

$$g(x,y) = \begin{cases} 1, & (x,y) \in A, \\ 0, & \text{otherwise.} \end{cases}$$

If the coordinates of the upper-left and lower-right corners of the rectangle describing the region are $(X_{\min}, Y_{\min})$ and $(X_{\max}, Y_{\max})$, respectively, then the area is

$$S = \sum_{y=Y_{min}}^{Y_{max}} \sum_{x=X_{min}}^{X_{max}} g(x,y).$$

The center of gravity of the region is given by the coordinates (X_c, Y_c), defined as the mean value (x, y) of the coordinates belonging to the region according to the equation

$$X_c = \frac{1}{S} \sum_{(x,y)\in A} x,$$

$$Y_c = \frac{1}{S} \sum_{(x,y)\in A} y.$$

Determining the coordinates of the center of gravity of the object allows one to normalize the position of the object by determining the position of the origin in the image plane. An object is given a central position.

If the number of end readings of a region is N, then the perimeter length P is the sum of the distances between the adjacent boundary points

$$P = \sum_{i=1}^{N} r_i,$$

$$r_i = \sqrt{(x_{i+1} - x_i)^2 + (y_{i+1} - y_i)^2}.$$

A reading is end if at least one of the nearest neighboring readings does not belong to the region A.

To assess the compactness of the object, a form factor is used, defined as the ratio of the perimeter square to the area

$$K = \frac{P^2}{S}.$$

To estimate the roundness of the region the following coefficient is used

$$C = \frac{m_A}{\sigma_A}.$$

where m_A – is the average value of the distances from the center of gravity of the region to the end readings, determined by the formula

$$m_A = \frac{1}{N}\sum_{i=1}^{N} r_{ic},$$

where σ_A – is spectral reflectance coefficient of these distances, determined by the formula

$$\sigma_A = \sqrt{\frac{1}{N-1}\sum_{i=1}^{N}(r_{ic} - m_A)^2},$$

where r_{ic} – is the distance from i end reading to the center of gravity of the region.

The radiuses of the inscribed and circumscribed circles are also used to assess the compactness of the object. Moreover, statistical moments of the region are often used for recognition.

The discrete central moment m_{ij} of a region is defined as follows

$$m_{ij} = \sum_{(x,y)\in \mathrm{Reg}} (x - \bar{x})^i (y - \bar{y})^j$$

$$\bar{x} = \frac{1}{n}\sum_{(x,y)\in \mathrm{Reg}} x,$$

$$\bar{y} = \frac{1}{n}\sum_{(x,y)\in \mathrm{Reg}} y,$$

where n – is the total number of pixels in the region.

Also, the scale, translation and rotation invariant features of the region are used, for recognition.

For example, eccentricity, characterizing elongation and eccentricity of an object

$$elongation = \frac{m_{20} + m_{02} + \sqrt{(m_{20} - m_{02})^2 + 4m_{11}^2}}{m_{20} + m_{02} - \sqrt{(m_{20} - m_{02})^2 + 4m_{11}^2}}.$$

A statistical approach is used to normalize the orientation of an object in analyzing binary images. The object is described by some scattering ellipse.

The direction of the eigenvector x of the covariance matrix B of the coordinates of non-zero brightness readings, that is, belonging to the region A is chosen for orientation.

The eigenvector must correspond to the maximum eigenvalue λ of covariance matrix

$$B = \begin{pmatrix} B_{11} & B_{12} \\ B_{22} & B_{21} \end{pmatrix},$$

where B_{ij} are central moments of the second order;

B_{11} is the dispersion of x- coordinates of non-zero brightness readings;

B_{22} is the dispersion of y- coordinates of non-zero brightness readings;

B_{12} is the covariance (x,y) of non-zero brightness readings coordinates.

The eigenvalues λ are found using the equation

$$(B - \lambda\ E)\ x_\lambda = 0,$$

where E is the unity matrix,

x_λ is the eigenvector corresponding to the number λ.

The eigenvalue λ of a covariance matrix is found using the equation

$$B - \lambda\, E = 0.$$

The parameters of the approximating ellipse estimated from the binary image are: the small half-axis a, the large half-axis b and the tilt angle of the ellipse major axis in accordance with the described statistical approach to the object binary image normalization.

The dimensions of the ellipse half-axes are defined as follows. The ratio of the covariance matrix eigenvalues (ellipse half-axes) is determined:

$$k = \sqrt{\frac{\mathrm{abs}(\lambda_2)}{\lambda_1}},$$

where λ_1 is the largest eigenvalue, λ_2 is the smallest eigenvalue.

If the ratio of the minor and major semi axes of the ellipse is $a / b = k$, then the area of the ellipse $Square = pab = pkb^2$.

The major half-axis of the ellipse is:

$$b = \sqrt{\frac{Square}{\pi k}},$$

where *Square* is the area of the binary image (the number of readings with non-zero brightness).

The minor half-axis of the ellipse is determined using the equation $a = kb$.

Satellite image classification technique.

The procedures for processing and analyzing satellite images include the following stages:

1) preprocessing (normalization) of satellite images, including orthorectification, augmentation of spatial resolution, radiometric enhancement, contour allocation;

2) thematic processing of normalized satellite images, including:

- converting to grayscale;
- thresholding binarization of the selected area;
- morphological filtering of binarized objects;
- segmentation of filtered binary objects;
- filtering of segmented objects by area;
- identification of geometric parameters;
- calculation of cross-correlation coefficient between geometric parameters;
- objects classification by geometric parameters taking into account a given threshold (nearness criterion);
- optimization of classification parameters in order to obtain the required number of classes;

- vectorization of recognized objects and exporting the results to a standard format.

The geometric features of the objects being classified in the binary image include:

- the area of the object (number of the object pixels);
- lengths of principle and auxiliary axes of inertia (the lengths of the axes, which represent the directions in the object corresponding to the semi-axes of inertia ellipsoid);
- the eccentricity of the object (eccentricity of an ellipse with principal moments of inertia equal to the principal moment of the object's inertia);
- the area of a polygon (the area of a convex polygon described near the object);
- equivalent diameter (diameter of a circle having the same area as the object; calculated using the formula *sqrt (4S/p)*, where *S* is the area of the object);
- object convexity coefficient (a coefficient that is equal to the ratio *S* / S*, where *S* is the area of the object; *S** is the area of the polygon).

Geometry-based classification of small-size objects assumes comparing all objects of the binary image following the each with each alignment algorithm by calculating the cross-correlation coefficient r between all values of the objects geometric features:

$$r = \frac{\frac{1}{n}\sum_{k=1}^{n}(x_{1k} - \overline{x_1})(x_{2k} - \overline{x_2})}{\sqrt{D_1 \cdot D_2}},$$

where x_1 and x_2 are mean values for two samples;

x_{1k} and x_{2k} – are the current sample values;

n – is the number of sample elements;

D_1 and D_2 – are the average variance for two samples.

Next, we set the threshold value of cross-correlation coefficient and select the pairs of objects which value is higher. We evaluate the obtained pairs of objects in order to combine them into classes on the basis of calculations results in a table form.

The threshold value of correlation coefficient depends on how much the objects combined into one class and the classes themselves differ from each other. Thus, the threshold value can be rough or insensitive to changes. Then in the limit case all objects are combined into one class. Or it can be more sensitive to the slightest differences between the objects. Then in the limit case several classes are created and only one object is added into each class. Therefore, to get the required number of classes it is very important to choose the optimal threshold value.

3 Results and Discussion

To research the automated object classification algorithm we used a fragment of a multispectral satellite sub-meter resolution image containing small moving objects. Preprocessing procedures included converting the original RGB image to grayscale and contour allocation (Fig. 1 and 2). This was followed by binarization, morphological filtering, segmentation and filtration by area (Fig. 3 and 4). Finally, we could obtain the image containing objects that were of interest for their subsequent classification.

Fig. 1. Original RGB image.

Fig. 2. Grayscale image.

Fig. 3. The result of binarization.

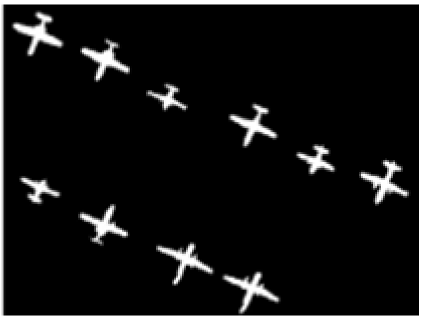

Fig. 4. The result of filtration by area.

Geometric features of all binary image objects were counted and normalized to one (Table 1).

Table 1. Geometric features of binary image objects.

Parameter	Object number									
	1	2	3	4	5	6	7	8	9	10
The area of the object	0.25	0.13	0.20	0.22	0.11	0.22	0.22	0.20	0.14	0.24
Length of the principle axis of inertia	0.84	0.67	0.83	0.86	0.67	0.95	0.94	0.81	0.65	0.78
Length of the auxiliary axis of inertia	0.69	0.46	0.59	0.60	0.43	0.63	0.63	0.68	0.50	0.76
The eccentricity of the object	0.56	0.72	0.70	0.71	0.76	0.74	0.73	0.54	0.63	0.23
The area of a polygon	0.52	0.25	0.46	0.48	0.26	0.55	0.55	0.49	0.28	0.53
Equivalent diameter	0.56	0.41	0.50	0.53	0.38	0.53	0.53	0.51	0.43	0.55
The coefficient of convexity	0.48	0.52	0.43	0.45	0.44	0.40	0.40	0.41	0.52	0.45

Based on the results of calculating cross-correlation coefficient between all values of the objects geometric parameters, it is easy to determine which objects belong to the same class with the selected threshold value of the correlation coefficient K, which determines each class boundaries.

If $K = 0.8$, then three classes are formed, i.e. the two closest in geometric characteristics classes of four classes are combined into one when $K = 0.95$. An object that has been allocated to a separate class when $K = 0.95$ moves to the first class when $K = 0.8$. When $K = 0.99$, the objects are combined into seven classes, as the second and third classes formed when $K = 0.95$ fall into five classes, and the first and fourth classes remain.

The high level of processing procedures automation and relative simplicity of the proposed technique ensures its implementation in the form of a geoinformation web service [17], which, compared to traditional software and hardware, has significant organizational, technical and economic advantages, such as:

- it works directly in the browser, which does not require installation of additional software;
- software and hardware independence, which ensures using this web service on mobile devices;
- the results of image processing are stored on the server, which allows all customers to use the web service regardless of their location;
- high economic efficiency (does not require purchase of powerful graphic stations and expensive software);
- minimum requirements for the end-user training (there is no need to spend time studying large and complex software packages).

The results of this research are included in the educational materials for lectures and laboratory classes being a part of the module "Ultra-high spatial resolution satellite images processing" for senior students of the Oles Honchar Dnipropetrovsk National University within the framework of the course "Remote sensing systems" and also used to prepare course and diploma papers. Students test the proposed technique experimentally using multispectral images of various Earth areas acquired by the existing RSS satellites.

4 Conclusion

A method for automated classification of moving objects using geometric features invariant to rotation was developed and tested. To classify small size objects by geometric features, all objects of the binary image were compared following the each with each alignment algorithm by calculating the cross-correlation coefficient between all values of the objects geometric features.

Special software was developed for experimental testing of the proposed technique. It ensures obtaining noise-free binary images and classifying filtered objects by geometric features in arbitrary orientation of the satellite image or separate objects, and constructing properties graphs for each object and each class at different threshold values of each class properties.

Experimental studies carried out on various satellite images confirmed that neither object orientation nor image rotation by an arbitrary angle considerably affect the result of classification (the probability of correct class recognition was in the range 0.97…0.99).

Directions for further research. Currently, the proposed technique is being tested using multispectral images of various parts of the Earth obtained from various ultra-high resolution optical-electronic satellites in order to determine the optimal processing parameters for the main types of modern onboard scanners, taking into account the region and shooting conditions. Moreover, a simplified version of this technique (without preprocessing procedures) is successfully tested using multispectral aerial images acquired in the visible and infrared spectral ranges.

5 Acknowledgments

This work was supported by the Ministry of Education and Science of the Russian Federation in the framework of the Federal target program «Research and development of priority directions of development of the scientific-technological complex of Russia for 2014-2020» (unique ID project RFMEFI60819X0274).

References

1. Chen, G., Hay, G.J., Carvalho L.M.T., Wulder M.A.: Object-based change detection. International Journal of Remote Sensing 33, 4434–4457 (2012).
2. Blaschke, T.: Object based image analysis for remote sensing. ISPRS Journal of Photogrammetry and Remote Sensing 65, 2–16 (2010).
3. Hussain, M., Chen, D., Cheng, A., Wei, H., Stanley, D.: Change detection from remotely sensed images: from pixel-based to object-based approaches. ISPRS Journal of Photogrammetry and Remote Sensing 80, 91–106 (2013).
4. Cheng, G., Han, J.: A survey on object detection in optical remote sensing images. ISPRS Journal of Photogrammetry and Remote Sensing 117, 11-28 (2016).
5. Van Etten, A.: Object Detection in Satellite Imagery, a Low Overhead Approach, Part I. Aug 31, 2016, https://medium.com/the-downlinq/object-detection-in-satellite-imagery-a-low-overhead-approach-part-i-cbd96154a1b7, last accessed 2020/01/19.
6. An, Z., Shi, Z., Teng, X., Yu, X., Tang, W.: An automated airplane detection system for large panchromatic image with high spatial resolution. Opt. Int. J. Light Electron Opt. 125, 2768–2775 (2014).
7. Yuan, J., Yang, H.H.L., Omitaomu, O.A., Bhaduri, B. L.: Large-scale solar panel mapping from aerial images using deep convolutional networks. In: Proceedings - 2016 IEEE International Conference on Big Data, pp. 2703–2708. IEEE, Washington, United States (2016).
8. Malof, J.M., Bradbury, K., Collins, L.M., Newell, R.G.: Automatic detection of solar photovoltaic arrays in high resolution aerial imagery. Applied Energy 183, 229-240 (2016).
9. Saito, S., Aoki, Y.: Building and road detection from large aerial imagery. In: Proceedings of Society of Photographic Instrumentation Engineers (SPIE) – The International Society of Optical Engineering, vol. 9405, art. 94050K. SPIE, San Francisco, United States (2015).

10. Chen, X., Xiang, S., Liu, C.L., Pan, C.H.: Vehicle detection in satellite images by hybrid deep convolutional neural networks. IEEE Geoscience and remote sensing letters 11(10), 1797-1801 (2014).
11. Audebert, N., Saux, B. L., Lefèvre, S.: Segment-before Detect: Vehicle Detection and Classification through Semantic Segmentation of Aerial Images. Remote Sensing 9(4), art. 368 (2017).
12. Razakarivony, S., Jurie, F.: Vehicle detection in aerial imagery: A small target detection benchmark. Journal of Visual Communication and Image Representation 34, 187-203 (2016).
13. Yuan, J.: Automatic building extraction in aerial scenes using convolutional networks, arXiv:1602.06564 (2016).
14. Shu, Y.: Deep Convolutional Neural Networks for Object Extraction from High Spatial Resolution Remotely Sensed Imagery, Ph.D. thesis, University of Waterloo (2014).
15. Saito, S., Yamashita, T., Aoki, Y.: Multiple object extraction from aerial imagery with convolutional neural networks. Journal of Imaging Science and Technology 60 (1), 010402 (2016).
16. Mozgovoj, D.K., Kravets, O.V.: A classification of the low-sized objects on high resolution satellite images. Ecology and noospherology 20(1-2), 26-31 (2009).
17. Mozgovoy, D.K., Tsarev, R.Y., Almabekova, O.A., Pupkov, A.N.: Satellite monitoring of the drought consequences via medium and high resolution multispectral images. In: 18th International Multidisciplinary Scientific Geoconference, SGEM 2018, vol. 18 (4.2), pp. 579-590. Albena, Bulgaria (2018).